Rheological response under non-isothermal stretching for immiscible blends of isotactic polypropylene and acrylate polymer

Jiraporn Seemork[1,2], Takumi Sako[1], Mohd Amran Bin Md Ali[1,3], and Masayuki Yamaguchi[1*]

[1] School of Materials Science, Japan Advanced Institute of Science and Technology
1-1 Asahidai, Nomi, Ishikawa 923-1292 JAPAN
[2] Program in Petrochemistry, Faculty of Science, Chulalongkorn University
Phayathai Rd., Bangkok 10330 THAILAND
[3] Department of Manufacturing Process, Faculty of Manufacturing Engineering,
Universiti Teknikal Malaysia Melaka
Hang Tuah Jaya, 76100 Durian Tunggal, Melaka, MALAYSIA.

*Corresponding author: M. Yamaguchi
Phone: +81-761-51-1621
Fax: +81-761-51-1149
E-mail address: m_yama@jaist.ac.jp

Synopsis

The addition of acrylate polymers with low molecular weight, such as poly(isobutyl methacrylate) PIBM and poly(methyl methacrylate) PMMA, effectively enhances the force required to stretch a molten polypropylene (PP) at the non-isothermal condition without the enhancement of shear viscosity in the molten state. The mechanism of this phenomenon is found to be attributed to prompt solidification of PIBM and PMMA droplets, which deform greatly to the flow direction in the die land and near the die exit during the extrusion and stretching processes. After the die exit, the deformed droplets show the glassification prior to the crystallization of PP matrix because of the rapid cooling at stretching. Consequently, they behave like rigid fibers in a molten PP, which provide the excess stress by large shear deformation of the matrix between the dispersed glassy fibers during stretching.

I. INTRODUCTION

Since the pioneering work was carried out by Meissner [1], elongational viscosity has been recognized as one of the most important rheological properties to decide the processability at various processing operations, in which free surface of a polymer melt is deformed. Along with the basic understanding by the theoretical approaches and the advanced experimental set-ups for the measurements [2-7], various techniques to enhance the elongational viscosity have been proposed.

One of the most well-known methods to enhance the elongational viscosity of a polymer melt is the addition of high molecular weight fraction [8,9]. Another well-known method is to incorporate long-chain branches by either in-reactor polymerization or postreactor operation. Low-density polyethylene (LDPE) produced by a radical polymerization process is the most well-known polymer having long-chain branches. The branch structure, which is decided by the polymerization method and the reactor type, greatly affects the rheological response under elongational flow [10,11]. In the last two decades, isotactic polypropylene (PP) having long-chain branches has been also developed by copolymerization of propylene and nonconjugated dienes by metallocene catalyst [12,13] and chemical reaction by peroxide and/or radiation [14-22]. According to them, PP with long-chain branches provides marked strain-hardening behavior in elongational viscosity, although the number of long-chain branches is much fewer than that in LDPE. Moreover, because the localized deformation is prohibited by the rapid increase in the stress by the deformation, they show good processability at thermoforming and extrusion foaming [17,18,21,23]. The marked strain-hardening in elongational viscosity is also responsible for the small level of neck-in at T-die film processing including extrusion-coating. Such types of PP have been already commercialized and known as HMS-PP (high-melt-strength PP) [14,24]. In contrast, polymers containing long-chain branches show extrudate distortion even at a low out-put rate

owing to the unsteady contraction flow at the reservoir-to-die area, which can be improved by the applied shear history, called shear modification [22,25-27].

In addition, mixing of rigid fibers with a large aspect ratio has been known to enhance the elongational viscosity of a molten polymer without an increase in the strain-hardening behavior, meaning that a composite shows high transient elongational viscosity in the whole time/strain region [28-33]. During uniaxial elongational deformation with a constant volume, excess localized shear deformation between neighboring fibers occurs, which is responsible for the stress increase. Therefore, the enhancement of elongational viscosity is pronounced especially for a dispersion containing long and thin fibers, which was theoretically derived by Batchelor [34].

Not only rigid fibers but also flexible fine fibers have the capability to affect the rheological response under elongational flow greatly for a polymer melt. The network structure composed of flexible fibers in a polymer melt can be deformed to the flow direction without losing the topological interaction between fibers because of their flexibility. Consequently, the frictional force between fibers and bending force of a part of fibers provide the excess stress, which is responsible for the strain-hardening in elongational viscosity [35-38].

Since the drawdown force, *i.e.*, the force required to stretch a melt uniaxially, has a close relationship with elongational viscosity, the drawdown force measurement is one good approach to evaluate the rheological responses of a molten polymer under uniaxial elongational flow [39-44]. Moreover, the processability is often predicted directly from the drawdown force, because the measurement is performed at the non-isothermal condition as similar to actual processing operations [3,18,40,44-46]. According to previous studies on the rheological properties for an immiscible polymer blend with sea-island structure, in which the dispersion has lower viscosity, the interfacial tension is known to barely affect the

elongational viscosity including the strain-hardening behavior [47-52]. To the best of our knowledge, moreover, it has been never reported that the drawdown force for a polymer is enhanced by an immiscible polymeric material with low molecular weight.

Here, a new method to enhance the drawdown force of PP at capillary extrusion is proposed; the addition of acrylate polymers with low molecular weight such as poly(isobutyl methacrylate) PIBM and poly(methyl methacrylate) PMMA. Since it is firstly reported that an immiscible linear polymer with low shear viscosity in the molten state can be used as a rheological modifier to enhance the drawdown force, this method would possess strong impact on industry.

II. EXPERIMENTAL

A. Materials and sample preparation

Two types of commercially available propylene homopolymer (PP) having different molecular weight (Japan Polypropylene, Japan), denoted as PP-H (M_n = 4.5 x10^4, M_w = 2.6 x 10^5, and M_w/M_n=5.8) and PP-M (M_n = 4.3 x 10^4, M_w = 2.1 x 10^5, and M_w/M_n=4.9), were employed in this study. Melt flow rates (MFR) of PP-H and PP-M are 5 and 10 g/10 min, respectively. In addition, a random polymer of polypropylene having 3 wt.% of ethylene content with 10 g/10 min of MFR (Prime Polymer, Japan), denoted as PP-random, was also used. Poly(isobuthyl methacrylate) PIBM and poly(methyl methacrylate) PMMA, kindly provided by Mitsubishi Rayon Co., Ltd., Japan, were used as the rheological modifiers. Both PIBM and PMMA are fully amorphous with linear structure. The number- and weight-average molecular weights are as follows: M_n = 1.6 x 10^4, M_w = 2.9 x 10^4, and M_w/M_n = 1.8 for PIBM and M_n = 1.8 x 10^4, M_w = 3.1 x 10^4, and M_w/M_n = 1.7 for PMMA, as a polystyrene standard.

The sample was prepared by melt-mixing of PP with 5 wt.% of either PIBM or PMMA using an internal batch mixer (Labo-Plastmill, Toyoseiki, Japan) with a blade rotational speed of 30 rpm at 200 °C for 3 minutes with the presence of 5,000 ppm of thermal stabilizers, such as tris(2,4-di-tert-butylphenyl)phosphate (Irgafos168, Ciba, Switzerland) and pentaerythritol tetrakis(3-(3,5-di-tert-butyl-4-hydroxyphenyl)propionate) (Irganox1010, Ciba, Switzerland). Then the mixed sample was compressed into a flat sheet at 230 °C for 3 minutes using a compression-molding machine (IMC-180C, Imoto, Japan) and subsequently quenched in the cooling unit. Some of the compressed sheets were cut into small pieces to evaluate the rheological properties by a capillary rheometer.

B. Measurements

A dynamic mechanical analyzer (E4000, UBM, Japan) was used to investigate the temperature dependence of oscillatory tensile moduli such as storage modulus *E'* and loss modulus *E"*. The measurement was performed in the temperature range between -80 and 170 °C at a heating rate of 2 °C/min. The applied frequency was 10 Hz. The measurements were performed twice without changing the sample to confirm that the samples are thermally stable.

A cone-and-plate rheometer (AR2000, TA Instruments, USA) was used to evaluate the frequency dependence of oscillatory shear moduli such as storage modulus *G'* and loss modulus *G"*. The measurements were performed at various temperatures such as 190, 210, 230 and 250 °C. The angle of a cone was 4° and the diameter was 25 mm. Furthermore, the rheometer was used to evaluate the steady-state shear stress and primary normal stress difference at 190 °C. To confirm the accuracy of the data, the measurements were performed twice without changing the sample.

The growth curves of uniaxial elongational viscosity were obtained by the rotational rheometer equipped with a universal testing platform (SER2-G, Xpansion Instruments, USA) at 190 °C. Rectangular samples with 10 mm wide, 15 mm long, and 0.5 mm thick were used.

The drawdown force, defined as the force required to stretch a polymer melt uniaxially, was measured using a capillary rheometer (140 SAS-2002, Yasuda Seiki Seisakusyo, Japan) equipped with dies having *L/D* ratios of 10/1 and 40/1. An entrance angle of the dies was 180°. A set of rotating wheels and a tension detector were attached to the capillary rheometer in order to evaluate the drawdown force at a constant draw ratio, *i.e.*, the ratio of the average flow velocity at the die exit to that at the rotating wheels. The draw ratio, *i.e.*, 2.4, was chosen to evaluate the value precisely. The apparatus was shown in our previous paper [45]. The applied shear rate and temperature in the die and reservoir were controlled at 124 s^{-1} and 190 °C, respectively. The distance between the die exit and the tension detector was 235 mm. Flow curve was investigated at various shear rates by the capillary rheometer at 190 °C using a die with an *L*/*D* of 10/1. In the case of the flow curve measurements, the diameter of an extruded strand was evaluated online without stretching a strand by means of a laser detector fixed 50 mm below the die.

Thermal properties were evaluated by a differential scanning calorimeter (DSC 820, Mettler-Toledo, USA). The sample was heated from 25 to 190 °C with a heating rate of 30 °C/min. Then, it was cooled down to 25 °C with various cooling rates, *i.e.*, 1, 3, 10, 30, 100 and 300 °C/min. We used a small amount of the sample, *i.e.*, approximately 2 mg, to avoid the effect of the thermal conductivity and heat capacity at the high cooling rate.

An X-ray diffractometer (R-AXIS IIc, Rigaku, Japan) was employed to investigate the molecular orientation of the extruded samples. The strands extruded from the dies with various lengths, *i.e.*, 10 and 40 mm, at a draw ratio of 4 were irradiated using a graphite monochromatized CuKα radiation beam focused via a 0.3 mm pinhole collimator with a flat

163 20×20 cm^2 imaging plate (IP) detector of 1,900 × 1,900 pixels. The sample was exposed to
164 the X-ray beam perpendicular to the strand axis in the through view direction for 7 min.
165 Morphology of the dispersed phase in PP matrix was observed using a scanning electron
166 microscope (SEM) (S400, Hitachi, Japan). The fractured surface in liquid nitrogen of a
167 compressed film was used for the SEM observation after sputter-coating. Moreover, the
168 deformation of the dispersed acrylate polymers in an extrudate was characterized by SEM.
169 The strand extruded from the die with an *L/D* ratio of 40/1 or 10/1 without stretching was cut
170 in the cross-section (end-view) and along the flow direction (side-view) using a razor blade.
171 Then, the cut sample was soaked into acetone for overnight to dissolve the acrylate polymer.
172 After sputter-coating of the dried sample, the cut surface was observed by SEM. Deformation
173 of the dispersed phase was further confirmed by the measurement of lateral expansion of a
174 strand after dipping into a silicone oil bath at 170 °C for 10 seconds.
175

176 **III. RESULTS AND DISCUSSION**

177 Fig. 1 shows the temperature dependence of oscillatory tensile moduli at 10 Hz with the
178 SEM image of the fractured surface for a compressed film of PP-H/PIBM (95/5). In the
179 figure, the *E"* curves of the pure components, *i.e.*, PP-H and PIBM, are plotted together in the
180 figure by the open symbols, which are shifted in the vertical direction to see the peaks clearly.
181 The peak temperatures in the *E"* curves ascribed to the glass-to-rubber transition for
182 individual pure polymers, *i.e.*, β-relaxation for PP-H and α-relaxation for PIBM, are 10 and
183 62 °C for PP-H and PIBM, respectively. As seen in the figure, there are double peaks in the
184 *E"* curve for the blend, which correspond with the individual peaks of the pure components,
185 *i.e.*, PP-H and PIBM. This result demonstrates that PP-H and PIBM are immiscible, as
186 demonstrated by the SEM picture. The diameter of the dispersed PIBM droplets is found to

be 0.5-3 μm. A similar result is obtained for the PP-H/PMMA blend. The diameter of PMMA droplets is 2-10 μm.

[FIG. 1]

Fig. 2 exemplifies the master curves of frequency dependence of oscillatory shear moduli for PP-H/PIBM (95/5), PP-H and PIBM at the reference temperature of 190 °C. The time-temperature superposition principle is applicable to all samples including the blends with acrylate polymers. Both moduli of PP-H/PIBM (95/5) are almost the same with those of the neat PP-H even though the blend shows phase-separated structure. Since the amount of the dispersed phase is only 5 wt.%, the contribution of interfacial tension to the moduli is negligible. The zero-shear viscosities η_0 at 190 °C obtained from the master curves are shown in Table I. As seen in the table, the viscosities of both PIBM and PMMA are much lower than those of PP samples at the extrusion temperature.

[FIG. 2]

Table I Zero-shear viscosity at 190 °C of the materials

Samples	η_0 at 190 °C
PP-H	9,850
PP-M	3,930
PP-random	4,930
PIBM	45
PMMA	280
PP-H/PIBM (95/5)	9,300
PP-H/PMMA (95/5)	9,500

Fig. 3 shows the shear stress and primary normal stress difference at the steady-state shear flow, evaluated by the cone-and-plate rheometer at 190 °C. As seen in the figure, both shear stress and normal stress difference for the blend are slightly lower than those of pure PP-H, although the difference is not so obvious. The slight decrease in the shear viscosity is

reasonable because of the low shear viscosity of PIBM at 190 °C (Table 1). Furthermore, the result corresponds with the oscillatory data.

[FIG. 3]

The flow curves at 190 °C for PP-H and PP-H/PIBM (95/5) are also evaluated by the capillary rheometer, as shown in Fig. 4. As similar to the result in Fig. 3, the shear viscosity of the blend is slightly lower than that of the neat PP-H at low shear rates. This is reasonable because PIBM has significantly lower shear viscosity than PP-H. Moreover, it is almost the same at high shear rates. The extrudate swell is also evaluated at this measurement (without stretching). It is found that there is no difference in the swell ratio. These results indicate that blending PIBM hardly affects the rheological responses of PP-H under shear flow at 190 °C.

[FIG. 4]

Fig. 5 shows the transient elongational viscosity as a function of time at various Hencky strain rates for PP-H/PIBM (95/5) at 190 °C. The solid line in the figure represents three times of the growth curve of shear viscosity in the linear region, *i.e.*, $3\eta^+$, which was calculated by the following equation proposed by Osaki *et al*. [53].

$$\eta^+(t) = t\left[G''(\omega) + 1.12G'(\omega/2) - 0.200G'(\omega)\right]_{\omega=1/t} \quad (1)$$

The upturn departure of elongational viscosity from the predicted values is not clearly detected for the blend, as similar to the neat PP-H (data not shown). In other words, the addition of the acrylate polymers does not provide strain-hardening behavior in the elongational viscosity.

It is concluded from Figs. 2-5 that the rheological responses of PP-H are barely affected by the addition of PIBM at least at 190 °C, which corresponds with previous reports [47-52].

[FIG. 5]

The drawdown force evaluated using two types of dies is shown in Fig. 6. It should be noted that the blend with an acrylate polymer exhibits a high value of the drawdown force,

which is more pronounced for the blend with PIBM. The enhancement is obvious when using the long die. This is a surprising result because the acrylate polymers with linear structure show much lower shear viscosity than PP, which will be discussed later.

[FIG. 6]

The enhancement of the drawdown force for crystalline polymers such as PP and HDPE is pronounced when using a long die as discussed in our previous works [45,46]. Because a flow history in a long die reduces the number of entanglement couplings with marked molecular orientation due to the prolonged exposure to high shear stress in a laminar flow in the die land, the crystallization takes place rapidly as the melt leaves the die, resulting in the steep increase in the elongational stress and thus, the drawdown force. Such phenomenon is pronounced for a system with long relaxation time. This behavior was confirmed by 2D X-ray diffraction (2D-XRD) patterns. Since the same phenomenon, *i.e.*, enhancement of the drawdown force, is detected for the present blends, the orientation of PP chains is examined. Fig. 7 shows the 2D-XRD patterns for the strand of PP-H and the blend extruded from the die with an L/D of 40/1. The strong peaks in equator, ascribed to the (040) plane of α-form monoclinic crystals, demonstrate that PP chains orient to the flow direction for both PP-H and the blend. Furthermore, the (110) plane of β-form crystals is detected near the (040) of α-form, which also shows the orientation in the flow direction. Moreover, it should be noted that the azimuthal intensity distribution becomes narrow for the strand of the blend, suggesting the high level of molecular orientation. The same XRD pattern was obtained for the blend with PMMA (but not present here).

[FIG. 7]

As the great enhancement of the drawdown force is observed for the blends with the acrylate polymers, further experiments were performed to clarify the mechanism. Since the marked molecular orientation of PP is detected for the blends, the nucleating ability of the

acrylate polymers was, then, studied by the DSC cooling curve as shown in Fig. 8. It is found that the crystallization temperatures T_c's of the blends are almost the same as that of the neat PP-H. This result indicates that the acrylate polymers have no nucleating ability at the crystallization of PP-H.

[FIG. 8]

Furthermore, the solidification behavior was studied at various cooling rates, because the drawdown force is measured at the rapid cooling condition. It has been well known that the cooling rate has strong impact on the T_c and glass transition temperature T_g of a polymer [54-58]. In general, both T_c and T_g decrease with increasing the cooling rate. Fig. 9 shows the effect of cooling rate on T_c of PP-H and T_g's of PIBM and PMMA, evaluated by DSC. As seen in the figure, T_c of PP-H is significantly sensitive to the cooling rate, because it drastically decreases with the cooling rate. The T_c values, including those obtained at the high cooling rates, well correspond with those reported previously, suggesting that the measurements were performed correctly [58,59]. In the case of PIBM and PMMA, in contrast, T_g's are found to be less sensitive to the cooling rate. Further, T_g of PMMA is located at a higher temperature than T_c of PP-H at a high cooling rate, *e.g.*, 300 °C/min, indicating that the solidification, *i.e.*, glassification, of PMMA takes place prior to the crystallization of PP-H at this condition. The actual cooling rate near the die exit at the capillary extrusion with melt stretching is considerably high. At the present experiment using PP-H, the freeze line was detected around at 10 mm below the die exit, suggesting that the cooling rate is higher than 100 °C/s, *i.e.*, > 6,000 °C/min. As a result, the steep increase in the viscosity of the acrylate polymers due to the glassification cannot be ignored. In fact, it has been reported that T_c of PP is around 60 °C in this range of the cooling rate [58-60]. Regarding the cooling rate at the non-isothermal melt spinning, Joo *et al*. [61] calculated to be about 50,000 °C/min by the numerical analysis, in which a similar condition to the present

study was assumed. Although the effect of the flow field on the crystallization behavior has to be taken into consideration, it is obvious that the acrylate polymer acts as high viscous or glassy dispersions in a molten PP at the non-isothermal stretching.

[FIG. 9]

Although the acrylate polymers do not show the nucleating ability for the crystallization of PP-H, they strongly affect the drawdown force. Since PIBM and PMMA possess low shear viscosity at the extrusion condition, they exist as dispersed liquid droplets in the PP matrix in the die. Therefore, the deformation of droplets in a matrix has to be considered to understand this interesting rheological behavior. In general, the size of droplets is determined by interfacial tension, viscosity ratio, and mixing conditions including stress, type of flow, and distributive performance. When the viscosity of droplets is much lower than that of a matrix with a relatively small interfacial tension, droplets deform into fibrous shape by the hydrodynamic force [62-66].

As shown in Fig. 10, both PIBM and PMMA deform to the flow direction, which is pronounced in the strand after passing through the long die. Considering that the strands in the figure were collected without stretching after the die exit, the result demonstrates that the deformation of droplets occurs, at least, in the die land by the applied shear stress for a long residence time in a laminar flow. Furthermore, the volume of a PIBM droplet is smaller than that of PMMA on average. Since the viscosity ratio between the matrix and dispersion for the PP/PIBM blend is larger than that for the PP/PMMA blend, this is presumably attributed to the lower interfacial tension between PP and PIBM. The weak cohesive energy due to low molecular weight may be also responsible for the fine dispersion of PIBM. Consequently, the deformed PIBM has higher aspect ratio, whereas PMMA droplets deform into ellipsoidal shape with low aspect ratio. Then, the deformed droplets will behave like rigid fillers because of the glassification as discussed previously. Regarding the flow type to produce fibrous

dispersion, uniaxial flow would be the most effective [66], although other types of flow also have the capability to deform the droplets to some degree.

[FIG. 10]

Although T_g of PMMA is higher than that of PIBM, the drawdown force enhancement is pronounced by the PIBM addition. This would be attributed to the number and shape of the droplets, i.e., fibrous shape with high aspect ratio. The elongational stress in a suspension containing rigid fibers was discussed by the theoretical and experimental approaches. Among them, the slender-body theory was successfully developed to predict the elongational stress considering the excess deformation of a matrix between fibers [34], which was experimentally proved by Mewis and Metzner [28] and Laun [31]. According to the slender-body theory, elongational viscosity η_E of a suspension with long slender particles depends on the aspect ratio as well as the volume fraction of the particulate dispersion as expressed in the following equation,

$$\eta_E = 3\eta_c + \frac{4}{3}\eta_c \frac{\phi_d \left(\frac{l}{d}\right)^2}{ln\left(\frac{\pi}{\phi_d}\right)} \tag{2}$$

where η_c is the shear viscosity of a continuous phase, ϕ_d is the volume fraction of the dispersion, and l/d is the length-to-diameter ratio of fibers.

As indicated by this theory, localized excess stress generated by large shear deformation of a matrix located between neighboring fibers is responsible for the enhancement of elongational stress of a suspension. Since the distance between neighboring fibers is determined by the number of fibers, fine fibers with a high aspect ratio provide high elongational stress on average at the same volume fraction. Therefore, the blend with PIBM, which has a lot of fine fibers with a high aspect ratio, exhibits high elongational stress. In

other words, PIBM has a great ability to enhance the drawdown force, as compared with PMMA.

Because the solidification temperature of polymers depends on various factors, such as flow field, size and shape of the extrudate, extrusion temperature, stretch ratio, and molecular characteristics, the drawdown force must be also sensitive to such conditions and material characteristics. Here, the proposed mechanism is further confirmed using PP-random, which has a lower T_c than PP homopolymer having a similar shear viscosity, *i.e.*, PP-M. T_c's evaluated by DSC at a cooling rate of 10 and 100 °C/min are 115.0 °C and 99.0 °C for PP-M and 92.7 °C and 76.6 °C for PP-random. As seen in Fig. 11, the enhancement of the drawdown force by blending both PIBM and PMMA is not so obvious when using PP-M. On the contrary, this phenomenon is clearly detected when using PP-random. Because PP-random has lower T_c than PP-M, the crystallization of PP-random after passing through a die must take place slower than that of PP-M. As a result, the matrix between fibers deforms greatly prior to the crystallization, resulting in the high level of the drawdown force, which is enhanced at the extrusion with a long die because of a high aspect ratio of dispersions. This result indicates that the prompt solidification of the fibrous dispersions of the acrylate polymer provides localized shear deformation of the PP melt between the neighboring acrylate fibers during uniaxial stretching, as explained by Laun [31]. As a result, excess stress is generated owing to the large localized shear deformation, which is responsible for the high level of drawdown force.

[FIG. 11]

The deformation of the dispersed phase in the non-stretched strand is further confirmed by measuring the lateral expansion of the strand after dipping into a silicone oil bath at 170 °C. Because the uniaxial stretching was performed, the strand has a cylindrical shape. After immersion into the bath, PP matrix as well as the dispersed phase is melted immediately.

Then, the interfacial tension tends to pull the dispersions back to the spherical shape. Therefore, prolonged dispersions provide high level of the lateral expansion as well as the vertical shrinkage. Based on this technique, the magnitude of the deformation is estimated from the lateral expansion of the strands. Since there is no dispersed phase in the pure PP system, the level of strand expansion for the pure PP is decided by the degree of chain orientation. It is found that the strand expansion of PP-M (1.52 for L/D=40/1) is slightly higher than that of PP-random (1.50 for L/D=40/1). Furthermore, the value of PP-random/PIBM is much larger than that of pure PP-random as shown in Fig. 12. This is reasonable because the interfacial tension between the matrix and dispersions dominantly decides the shrinkage of the strands. Moreover, the strand expansion of the blend with PP-random is found to be significantly larger than that with PP-M, which correlates with the drawdown force enhancement. Considering that the drawdown force enhancement by the acrylate polymers is pronounced for PP-random, especially when using a long die, PIBM and PMMA droplets deform greatly in PP-random rather than in PP-M. This is owing to the slow solidification of PP-random, demonstrating that the deformation of the dispersions occurs even after passing through the die, which results in the high level of drawdown force.

[FIG. 12]

At present, we are studying the effect of material characteristics such as blend ratio, interfacial tension, and molecular weight on the rheological properties and processability at various processing operations. Furthermore, the effect of the die shape and entrance angle should be investigated considering the industrial applications. Besides, not only rheological properties but also mechanical properties in the solid state are interesting for the present blend system. As well known, the addition of liquid crystalline polymers affects mechanical properties for flexible polymers greatly [67-69]. Furthermore, oriented polymers obtained by flow-induced crystallization show marked rigidity [70-72]. Therefore, the mechanical

properties in the solid state of this blend system, considering the molecular orientation as well as the orientation of acrylate fibers, are worth for studying.

IV. CONCLUSION

Drawdown force enhancement of PP at capillary extrusion is demonstrated by blending immiscible acrylate polymers such as PIBM and PMMA, which have significantly low shear viscosity at the processing temperature of PP. It will be a new method to enhance the drawdown force for PP without an increase in the shear viscosity in an extruder. The mechanism of this phenomenon is found to be attributed to the prompt solidification of PIBM and PMMA at the rapid cooling condition like the drawdown force measurement. The dispersed droplets of the acrylate polymers deform to the flow direction in and near the die, which is determined by the die geometry, interfacial tension with PP, and viscosity ratio. Once their solidification takes place, they will act as rigid fibers. This situation occurs by the difference in the cooling rate dependence of solidification temperatures; *i.e.*, the crystallization temperature of PP is more sensitive to the cooling rate than the glass transition temperature of the acrylate polymers. Consequently, the drawdown force is enhanced by the excess stress generated by large shear deformation of a matrix between the solidified fibers. Considering that most processing operations are carried out at rapid cooling conditions, this phenomenon can be applicable to improve the processability.

Acknowledgements

The authors would like to thank Mitsubishi Rayon Co., Ltd., Japan Polypropylene Corp., and Prime Polymer Co., Ltd. for their kind support of the materials.

References

406 [1] Meissner, J., "Dehnungsverhalten von polyäthylen-schmelzen," Rheol. Acta **10**, 230-242
407 (1971).
408 [2] McLeish, T. C. B., and R. G. Larson, "Molecular constitutive equations for a class of
409 branched polymers: The pom-pom polymer," J. Rheol. **42**, 81-110 (1998).
410 [3] Wagner, M. H., H. Bastian, A. Bernnat, S. Kurzbeck, and C. Chai, "Determination of
411 elongational viscosity of polymer melts by RME and rheotens experiments," Rheol.
412 Acta **41**, 316-325 (2002).
413 [4] Sentmanat, M., "Miniature universal testing platform: From extensional melt rheology to
414 solid-state deformation behavior," Rheol. Acta **43**, 657-669 (2004).
415 [5] Münstedt, H., and D. Auhl, "Rheological measuring techniques and their relevance for
416 the molecular characterization of polymers," J. Non-Newtonian Fluid Mech. **128**, 62-69
417 (2005).
418 [6] Nielsen, J. K., H. K. Rasmussen, O. Hassager, and G. H. McKinley, "Elongational
419 viscosity of monodisperse and bidisperse polystyrene melts," J. Rheol. **50**, 453-476
420 (2006).
421 [7] Hawke, L. G. D., Q. Huang, O. Hassager, and D. J. Read, "Modifying the pom-pom
422 model for extensional viscosity overshoots," J. Rheol. **59**, 995-1017 (2015).
423 [8] Linster, J. J., and J. Meissner, "Melt elongation and structure of linear polyethylene
424 (HDPE)," Polym. Bull. **16**, 187-194 (1986).
425 [9] Sugimoto, M., Y. Masubuchi, J. Takimoto, and K. Koyama, "Melt rheology of
426 polypropylene containing small amounts of high-molecular-weight chain. 2. Uniaxial
427 and biaxial extensional flow," Macromolecules **34**, 6056-6063 (2001).
428 [10] Meissner, J., "Basic parameters, melt rheology, processing and end-use properties of
429 three similar low density polyethylene samples," Pure Appl. Chem. **42**, 551-621 (1975).

[11] Yamaguchi, M., and M. Takahashi, "Rheological properties of low-density polyethylenes produced by tubular and vessel processes," Polymer **42**, 8663-8670 (2001).

[12] Ye, Z., F. Al Obaidi, and S. Zhu, "Synthesis and rheological properties of long-chain-branched isotactic polypropylenes prepared by copolymerization of propylene and nonconjugated dienes," Ind. Eng. Chem. Res. **43**, 2860-2870 (2004).

[13] Langston, J. A., R. H. Colby, T. C. M. Chung, F. Shimizu, T. Suzuki, and M. Aoki, "Synthesis and characterization of long chain branched isotactic polypropylene via metallocene catalyst and T-reagent," Macromolecules **40**, 2712-2720 (2007).

[14] Phillips, E. M., K. E. Mchugh, and M. B. Bradley, "High performance polypropylene extrusion coating resins," J. Coated Fabrics **19**, 155-168 (1990).

[15] Hingmann, R., and B. L. Marczinke, "Shear and elongational flow properties of polypropylene melts," J. Rheol. **38**, 573-587 (1994).

[16] Yoshii, F., K. Makuuchi, S. Kikukawa, T. Tanaka, J. Saitoh, and K. Koyama, "High-melt-strength polypropylene with electron beam irradiation in the presence of polyfunctional monomers," J. Appl. Polym. Sci. **60**, 617-623 (1996).

[17] Park, C. B., and L. K. Cheung, "A study of cell nucleation in the extrusion of polypropylene foams," Polym. Eng. Sci. **37**, 1-10 (1997).

[18] Lau, H. C., S. N. Bhattacharya, and G. J. Field, "Melt strength of polypropylene: Its relevance to thermoforming," Polym. Eng. Sci. **38**, 1915-1923 (1998).

[19] Lagendijk, R. P., A. H. Hogt, A. Buijtenhuijs, and A. D. Gotsis, "Peroxydicarbonate modification of polypropylene and extensional flow properties," Polymer **42**, 10035-10043 (2001).

[20] Auhl, D., J. Stange, H. Münstedt, B. Krause, D. Voigt, A. Lederer, U. Lappan, and K. Lunkwitz, "Long-chain branched polypropylenes by electron beam irradiation and their rheological properties," Macromolecules **37**, 9465-9472 (2004).

[21] Spitael, P., and C. W. Macosko, "Strain hardening in polypropylenes and its role in extrusion foaming," Polym. Eng. Sci. **44**, 2090-2100 (2004).

[22] Yamaguchi, M., and M. H. Wagner, "Impact of processing history on rheological properties for branched polypropylene," Polymer **47**, 3629-3635 (2006).

[23] Stange J., and H. Münstedt, "Rheological properties and foaming behavior of polypropylenes with different molecular strcutures," J. Rheol. **50**, 907-923 (2006).

[24] Bradley, M. B., and E. M. Phillips, "Novel polypropylenes for foaming on conventional equipment," Plastics Eng. 82-84 (1991).

[25] Yamaguchi, M., D. B. Todd, and C. G. Gogos, "Rheological properties of LDPE processed by conventional processing machines," Adv. Polym. Technol. **22**, 179-187 (2003).

[26] Doelder, J., R. Koopmans, M. Dees, and M. Mangnus, "Pressure oscillation and periodic extrudate distortion of long-chain branched polyolefins," J. Rheol. **49**, 113-126 (2005).

[27] Siriprumpoonthum, N. Mieda, V. A. Doan, S. Nobukawa, and M. Yamaguchi, "Effect of shear history on flow instability at capillary extrusion for long-chain branched polyethylene," J. Appl. Polym. Sci., **124**, 429-435 (2012).

[28] Mewis, J., and A. B. Metzner, "The rheological properties of suspensions of fibres in Newtonian fluids subjected to extensional deformations," J. Fluid Mech. **62**, 593-600 (1974).

[29] Chan, Y., J. L. White, and Y. Oyanagi, “A fundamental study of the rheological properties of glass-fiber-reinforced polyethylene and polystyrene melts,” J. Rheol. **22**, 507-524 (1978).

478 [30] Kamal, M. R., A. T. Mutel, and L. A. Utracki, "Elongational behavior of short glass
479 fiber reinforced polypropylene melts," Polym. Comp. **5**, 289-298 (1984).
480 [31] Laun, H. M., "Orientation effects and rheology of short glass fiber-reinforced
481 thermoplastics," Colloid Polym. Sci. **262**, 257-269 (1984).
482 [32] Takahashi, T., J. Takimoto, and K. Koyama, "Uniaxial elongational viscosity of various
483 molten polymer composites," Polym. Comp. 20, 357-366 (1999).
484 [33] Thomasset, J., P. J. Carreau, B. Sanschagrin, and G. Ausias, "Rheological properties of
485 long glass fiber filled polypropylene," J. Non-Newtonian Fluid Mech. **125**, 25-34
486 (2005).
487 [34] Batchelor, G. K., "The stress generated in a non-dilute suspension of elongated particles
488 by pure straining motion," J. Fluid Mech. **46**, 813-829 (1971).
489 [35] Yokohara, T., S. Nobukawa, and M. Yamaguchi, "Rheological properties of polymer
490 composites with flexible fine fibers," J. Rheol. **55**, 1205-1218 (2011).
491 [36] Yamaguchi, M., K. Fukuda, T. Yokohara, M. A. B. M. Ali, and S. Nobukawa,
492 "Modification of rheological properties under elongational flow by addition of
493 polymeric fine fibers," Macromol. Mater. Eng. **297**, 654-658 (2012).
494 [37] Yamaguchi, M., T. Yokohara, and M. A. Bin Md Ali, "Effect of flexible fibers on
495 rheological properties of poly(lactic acid) composites under elongational flow," J. Soc.
496 Rheol. Jpn. **41**, 129-135 (2013).
497 [38] Rizvi, A., C. B. Park, and B. D. Favis, "Tuning viscoelastic and crystallization
498 properties of polypropylene containing in-situ generated high aspect ratio polyethylene
499 terephthalate fibrils," Polymer **68**, 83-91 (2015).
500 [39] Laun, H. M., and H. Schuch, "Transient elongational viscosities and drawability of
501 polymer melts," J. Rheol. **33**, 119-175 (1989).

[40] Bernnat, A., "Polymer melt rheology and the rheotens test," Ph.D. Thesis, University of Stuttgart, Stuttgart, Germany, (2001).

[41] Muke, S., I. Ivanov, N. Kao, and S. N. Bhattacharya, "Extensional rheology of polypropylene melts from the rheotens test," J. Non-Newtonian Fluid Mech. **101**, 77-93 (2001).

[42] Yamaguchi, M., "Melt elasticity of polyolefins: Impact of elastic properties on foam processing," Polymeric Foam (CRC Press, New York, 2004).

[43] Münstedt, H., T. Steffl, and A. Malmberg, "Correlation between rheological behaviour in uniaxial elongation and film blowing properties of various polyethylenes," Rheol. Acta **45**, 14-22 (2005).

[44] Gupta Rahul, K., and S. N. Bhattacharya, "The effect of die geometries and extrusion rates on melt strength of high melt strength polypropylene," J. Polym. Eng. **27**, 89-106 (2007).

[45] Seemork, J., M. Siriprumpoonthum, Y. Lee, S. Nobukawa, and M. Yamaguchi, "Effect of die geometry on drawdown force of polypropylene at capillary extrusion," Adv. Polym. Technol. **34**, 21477 (1-7) (2015).

[46] Seemork, J., T. Itoh, S. Nobukawa, and M. Yamaguchi, "Effect of crystallization on drawdown force at capillary extrusion for polyethylene," J. Soc. Rheol. Jpn. **44**, 23-27 (2016).

[47] Min, K., J. L. White, and J. F. Fellers, "High density polyethylene/polystyrene blends: Phase distribution morphology, rheological measurements, extrusion, and melt spinning behavior," J. Appl. Polym. Sci. **29**, 2117-2142 (1984).

[48] Utracki, L. A., and P. Sammut, "On the uniaxial extensional flow of polystyrene/polyethylene blends," Polym. Eng. Sci. **30**, 1019-1026 (1990).

526 [49] Hattori, T., T. Takigawa, and T. Masuda, “Uniaxial and biaxial elongational flow of low
527 density polyethylene/polystyrene blends,” J. Soc. Rheol. Jpn. **20**, 141-145 (1992).
528 [50] Gramespacher, H. and J. Meissner, “Melt elongation and recovery of polymer blends,
529 morphology, and influence of interfacial tension,” J. Rheol. **41**, 27-44 (1997).
530 [51] Takahashi, T., J. Takimoto, and K. Koyama, "Elongational vioscosity for miscible and
531 immiscible polymer blends. 1. PMMA and PS with similar elongational viscosity," J.
532 Appl. Polym. Sci., **73**, 757-766 (1999).
533 [52] Handge, U. A. and P. Pötschke, “Interplay of rheology and morphology in melt
534 elongation and subsequent recovery of polystyrene/poly(methyl methacrylate) blends”,
535 J. Rheol., **48**, 1103-1122 (2004).
536 [53] Osaki, K., A. Murai, N. Bessho, and B. S. Kim, "Linear viscoelastic relation concerning
537 shear stresses at the start and cessation of steady shear flow," J. Soc. Rheol. Jpn. **4**, 166-
538 169 (1976).
539 [54] Moynihan, C. T., A. J. Easteal, J. Wilder, and J. Tucker, "Dependence of the glass
540 transition temperature on heating and cooling rate," J. Phys. Chem. **78**, 2673-2677
541 (1974).
542 [55] Wasiak, A., P. Sajkiewicz, and A. Woźniak, "Effects of cooling rate on crystallinity of i-
543 polypropylene and polyethylene terephthalate crystallized in nonisothermal conditions,"
544 J. Polym. Sci. Polym. Phys. **37**, 2821-2827 (1999).
545 [56] Buchholz, J., W. Paul, F. Varnik, and K. Binder, "Cooling rate dependence of the glass
546 transition temperature of polymer melts: Molecular dynamics study," J. Chem. Phys.
547 **117**, 7364-7372 (2002).
548 [57] Mark, J., K. Ngai, W. Graessley, L. Mandelkern, E. Samulski, J. Koenig, and G.
549 Wignall, Physical Properties of Polymers (Cambridge University Press, Cambridge,
550 2004).

551 [58] Gradys, A., P. Sajkiewicz, A. A. Minakov, S. Adamovsky, C. Schick, T. Hashimoto, and
552 K. Saijo, "Crystallization of polypropylene at various cooling rates," Mater. Sci. Eng. A
553 **413–414**, 442-446 (2005).
554 [59] Schawe, J. E. K., "Analysis of non-isothermal crystallization during cooling and
555 reorganization during heating of isotactic polypropylene by fast scanning DSC,"
556 Thermochim. Acta **603**, 85-93 (2015).
557 [60] Mollova, A., R. Androsch, D. Mileva, M. Gahleitner, and S. S. Funari, "Crystallization
558 of isotactic polypropylene containing beta-phase nucleating agent at rapid cooling," Eur.
559 Polym. J. **49**, 1057-1065 (2013).
560 [61] Joo, Y. L., J. Sun, M. D. Smith, R. C. Armstrong, R. A. Brown, and R. A. Ross, "Two-
561 dimensional numerical analysis of non-isothermal melt spinning with and without phase
562 transition," J. Non-Newtonian Fluid Mech. **102**, 37-70 (2002).
563 [62] Macosko, C. W., Rheology: Principles, Measurements, and Applications (John Wiley &
564 Sons, New York, 1994).
565 [63] Larson, R. G., The Structure and Rheology of Complex Fluids (Oxford University Press,
566 New York, 1998).
567 [64] Hayashi, R., M. Takahashi, H. Yamane, H. Jinnai, and H. Watanabe, "Dynamic
568 interfacial properties of polymer blends under large step strains: Shape recovery of a
569 single droplet," Polymer **42**, 757-764 (2001).
570 [65] Tucker, C. L., and P. Moldenaers, "Microstructural evolution in polymer blends," Annu.
571 Rev. Fluid Mech. **34**, 177-210 (2002).
572 [66] Manas-Zloczower, I., Mixing and Compounding of Polymers: Theory and Practice (Carl
573 Hanser, Munich, 2009).

574 [67] Weiss, R. A., W. Huh, and L. Nicolais, “Novel reinforced polymers based on blends of
575 polystyrene and a thermotropic liquid crystalline polymer,” Polym. Eng. Sci., **27**, 684-
576 691 (1987).
577 [68] Dutta, D., H. Fruitwala, A. Kohli, and R. A. Weiss, "Polymer blends containing liquid
578 crystals: A review," Polym. Eng. Sci. **30**, 1005-1018 (1990).
579 [69] Tjong, S. C., S. L. Liu, and R. K. Y. Li, "Mechanical properties of injection moulded
580 blends of polypropylene with thermotropic liquid crystalline polymer," J. Mater. Sci. **31**,
581 479-484 (1996).
582 [70] Odell, J. A., D. T. Grubb, and A. Keller, "A new route to high modulus polyethylene by
583 lamellar structures nucleated onto fibrous substrates with general implications for
584 crystallization behavior," Polymer **19**, 617-626 (1978).
585 [71] Barham, P. J., Structure and Morphology of Oriented Polymer, in Structure and
586 Properties of Oriented Polymers, 2nd Ed., Ward, I. M. (Chapman & Hall, London, 1997).
587 [72] Tenma, M. and M. Yamaguchi, “Structure and properties of injection-molded
588 polypropylene with sorbitol-based clarifier,” Polym. Eng. Sci., **47**, 1441-1446 (2007).
589

590 **Figure captions**

591

592 FIG. 1. Temperature dependence of oscillatory tensile moduli such as storage modulus *E'*
593 (closed circles) and loss modulus *E"* (closed diamonds) for PP-H/PIBM (95/5) at 10 Hz. The
594 *E"* curves for pure PP-H (open circles) and pure PIBM (open diamonds) are also plotted with
595 a vertical shift (a = -1). An SEM image of cryogenically fractured surface of the compressed
596 film is also shown.

597

598 FIG. 2. Master curves of frequency dependence of oscillatory shear moduli such as storage
599 modulus *G'* (circles) and loss modulus *G"* (diamonds) for PP-H/PIBM (95/5) (closed
600 symbols), PP-H (open symbols), and PIBM (gray symbols) at the reference temperature of
601 190 °C.

602

603 FIG. 3. Steady-state shear stress σ (open symbols) and primary normal stress difference N_{11}
604 (closed symbols) for PP-H (circles) and PP-H/PIBM (95/5) (diamonds) at 190 °C. The data
605 for the blend are plotted with a horizontal shift (a = 1).

606

607 FIG. 4 Shear viscosity as a function of shear rate for PP-H (circles) and PP-H/PIBM (95/5)
608 (diamonds) at 190 °C.

609

610 FIG. 5. Transient elongational viscosity as a function of time at various Hencky strain rates at
611 190 °C for PP-H/PIBM (95/5). The solid line represents $3\eta^+(t)$ calculated from the
612 oscillatory shear modulus.

613

614 FIG. 6. Drawdown force of PP-H, PP-H/PIBM (95/5), and PP-H/PMMA (95/5) at a draw
615 ratio of 2.4. The applied shear rate at the die wall was 124 s^{-1} and the temperature was
616 controlled at 190 °C.
617
618 FIG. 7. 2D-XRD patterns for the strand of PP-H and PP-H/PIBM (95/5) extruded from the
619 dies having L/D = 40/1 at 190 °C and stretched at a draw ratio of 4. The plot below each
620 image represents the azimuthal intensity distribution of (040) plane, indicated by the arrows
621 in the image.
622
623 FIG. 8. DSC cooling curves for PP-H, PP-H/PIBM (95/5), and PP-H/PMMA (95/5) at a
624 cooling rate of 10 °C/min.
625
626 FIG. 9. Crystallization temperature T_c for PP-H (open circles) and glass transition
627 temperature T_g's for PIBM (closed squares) and PMMA (closed diamonds) as a function of
628 cooling rate.
629
630 FIG. 10. SEM pictures of the cut surface of the strands for PP-H/PIBM (95/5) and PP-
631 H/PMMA (95/5) extruded from a die with L/D = 10/1 or 40/1 without stretching; (a) end-
632 view, (b) center area of side-view, and (c) edge area of side-view. The cut surface was
633 immersed in acetone to remove the acrylate polymers. The arrows in the images represent the
634 flow direction.
635
636 FIG. 11. Drawdown force for the blends with 5 wt% of PIBM or PMMA stretched at a draw
637 ratio of 2.4. The temperature was controlled at 190 °C.
638

639 FIG. 12. Ratio of the strand diameter after dipping into silicone oil bath at 170 °C to that of
640 the original one for the blends of PP-M and PP-random with 5 wt% of PIBM and PMMA.
641 The strands were not stretched.

642

643 Table I. Zero-shear viscosity at 190 °C of the materials.

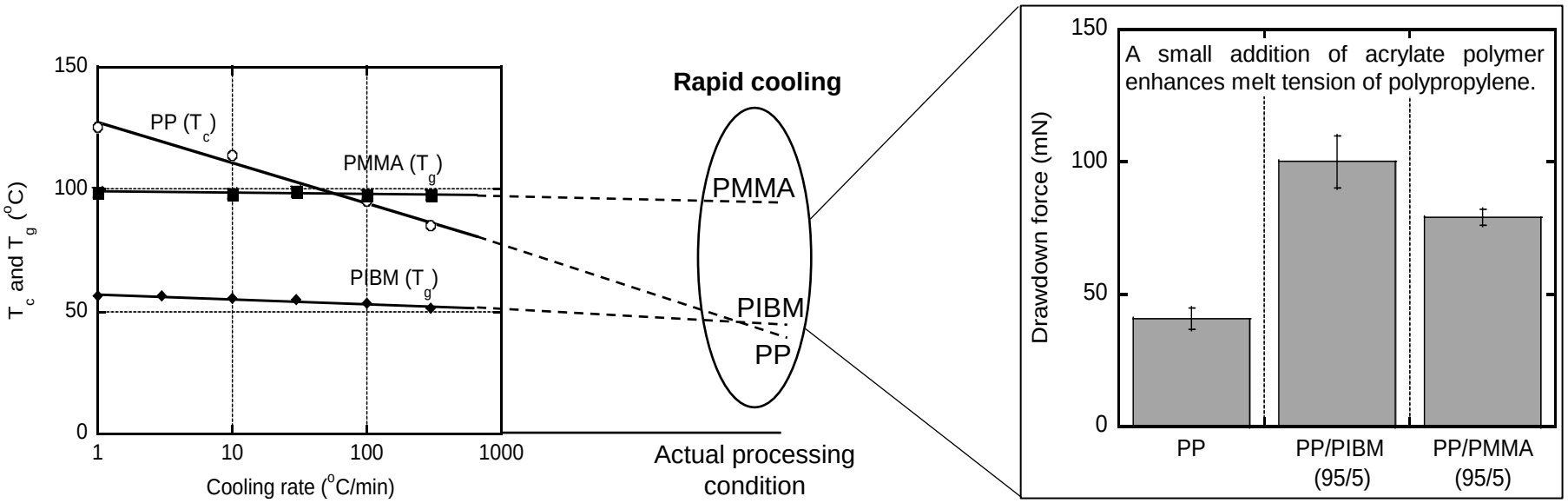

Prompt glassification of acrylate polymer with fibrous shape at rapid cooling → Localized deformation of PP melt → Enhancement of drawdown force (melt tension)

SEEMORK et al., Graphical abstract

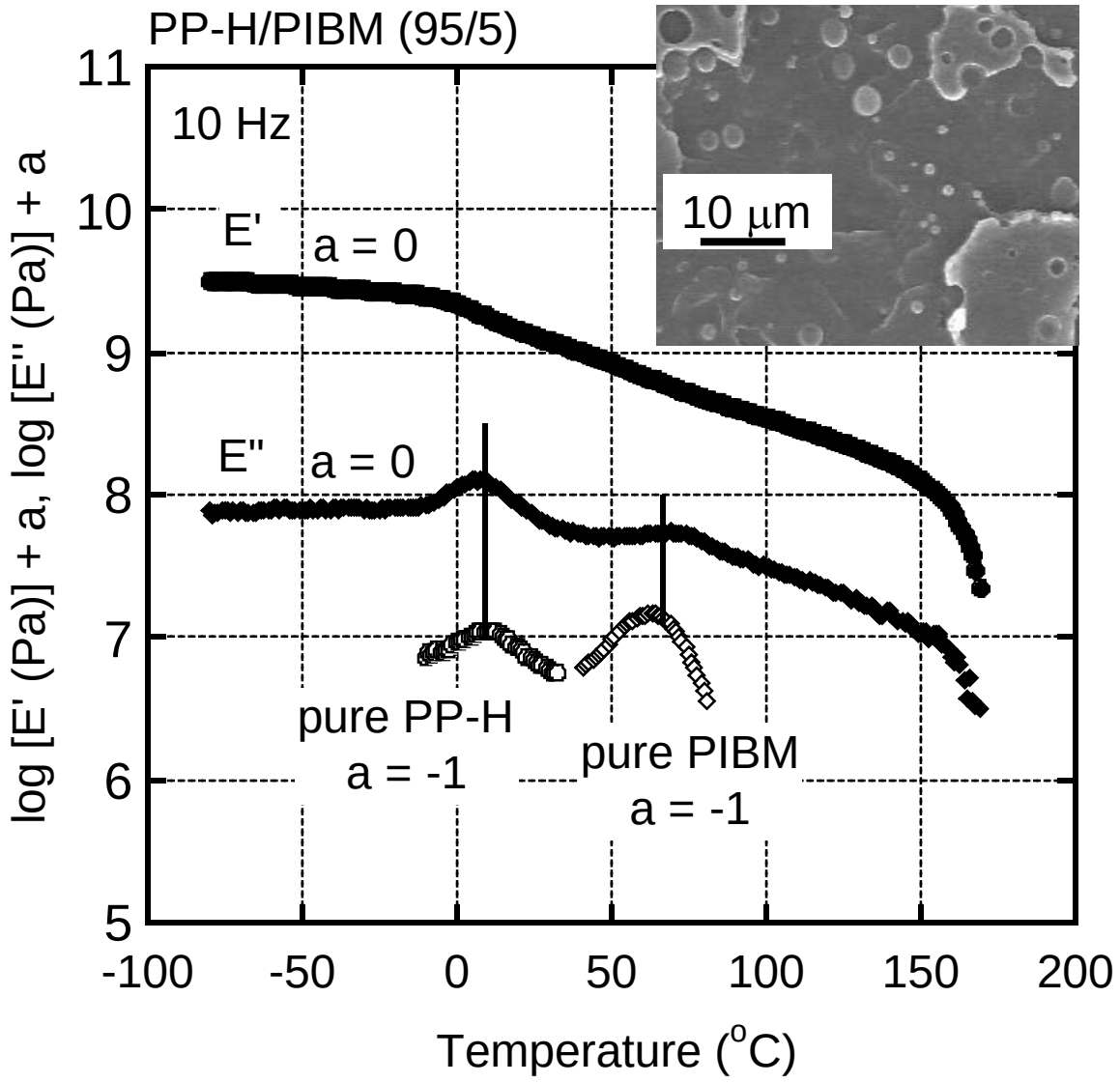

SEEMORK et al., FIG. 1

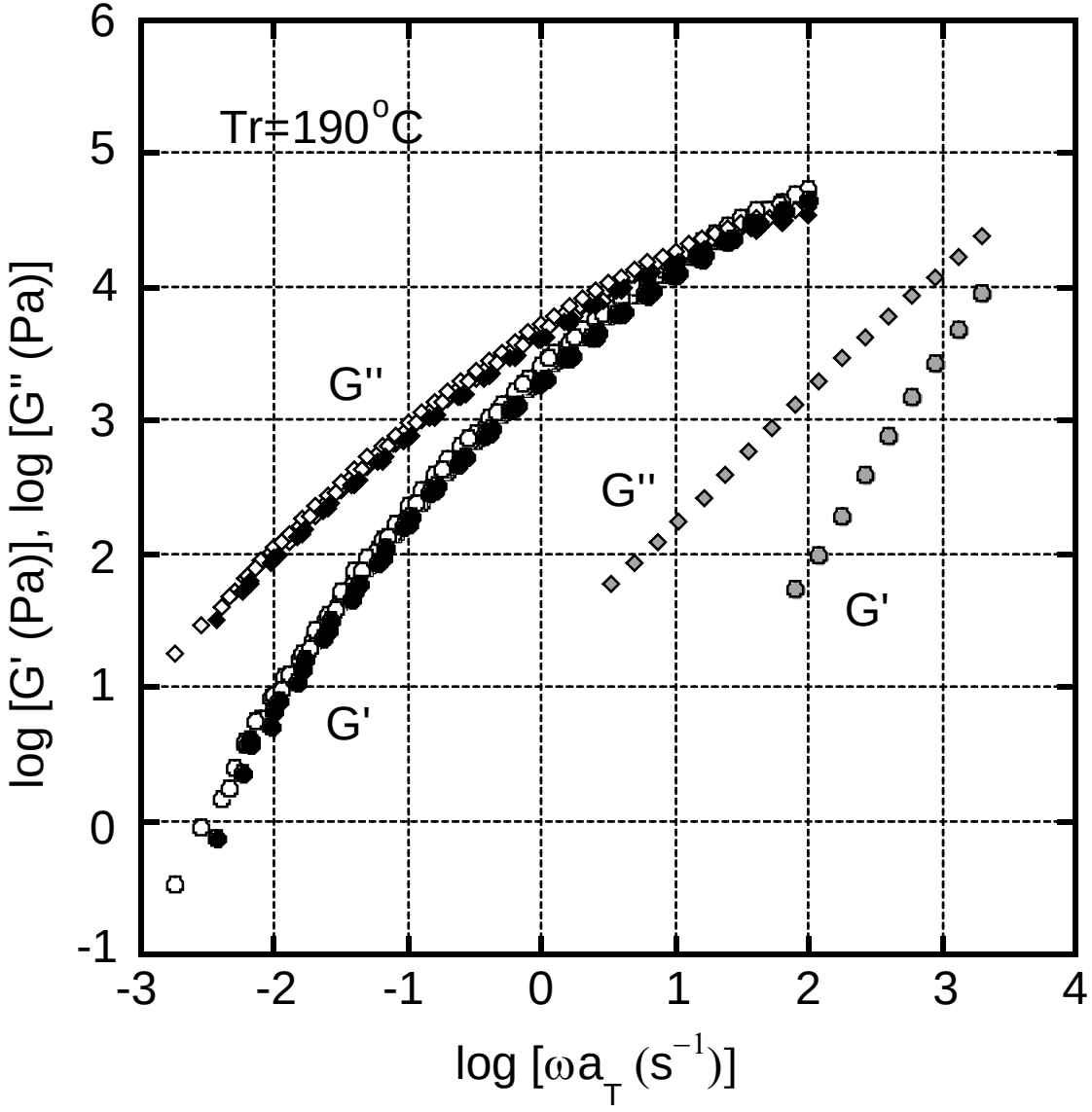

SEEMORK et al., FIG. 2

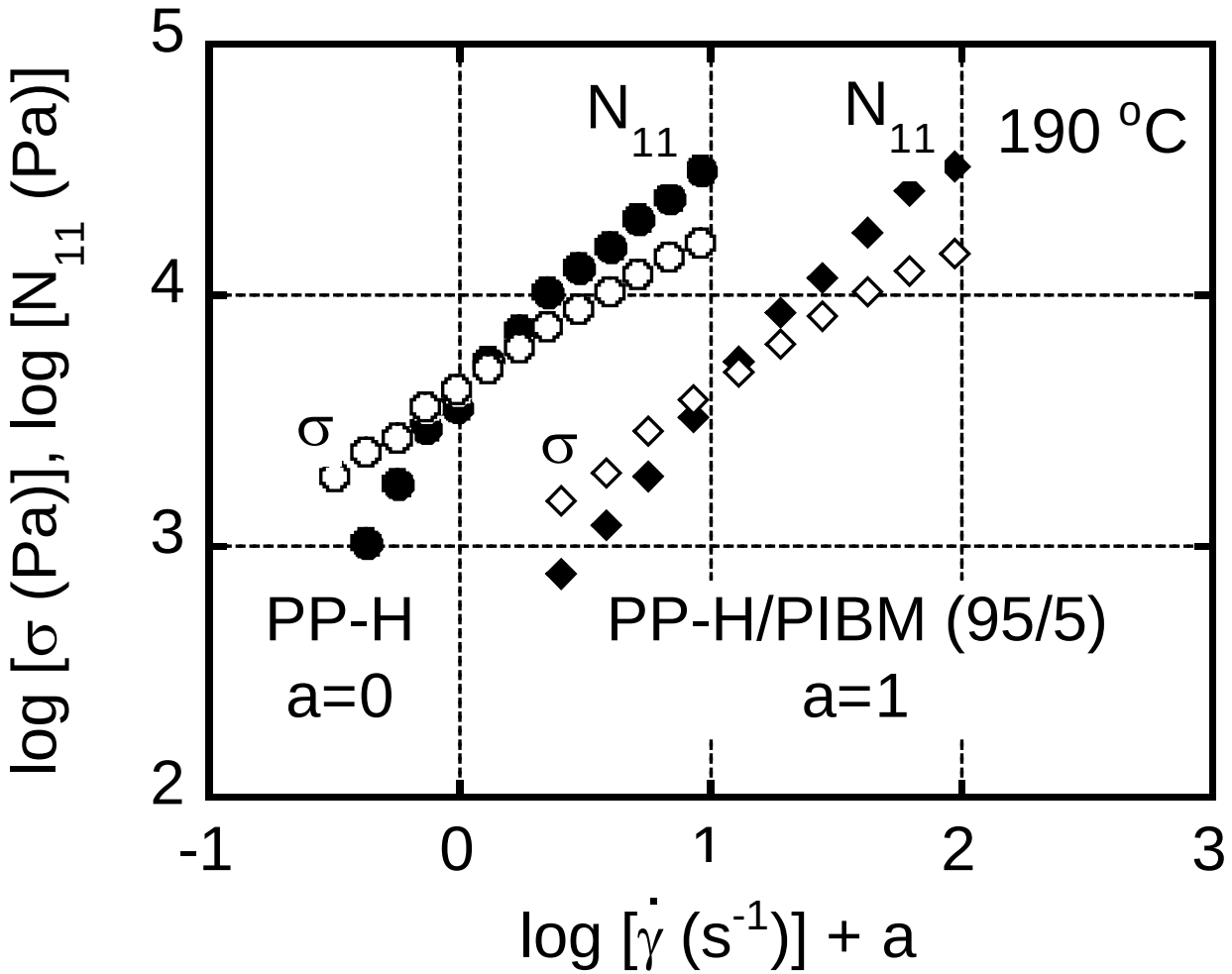

SEEMORK et al., FIG. 3

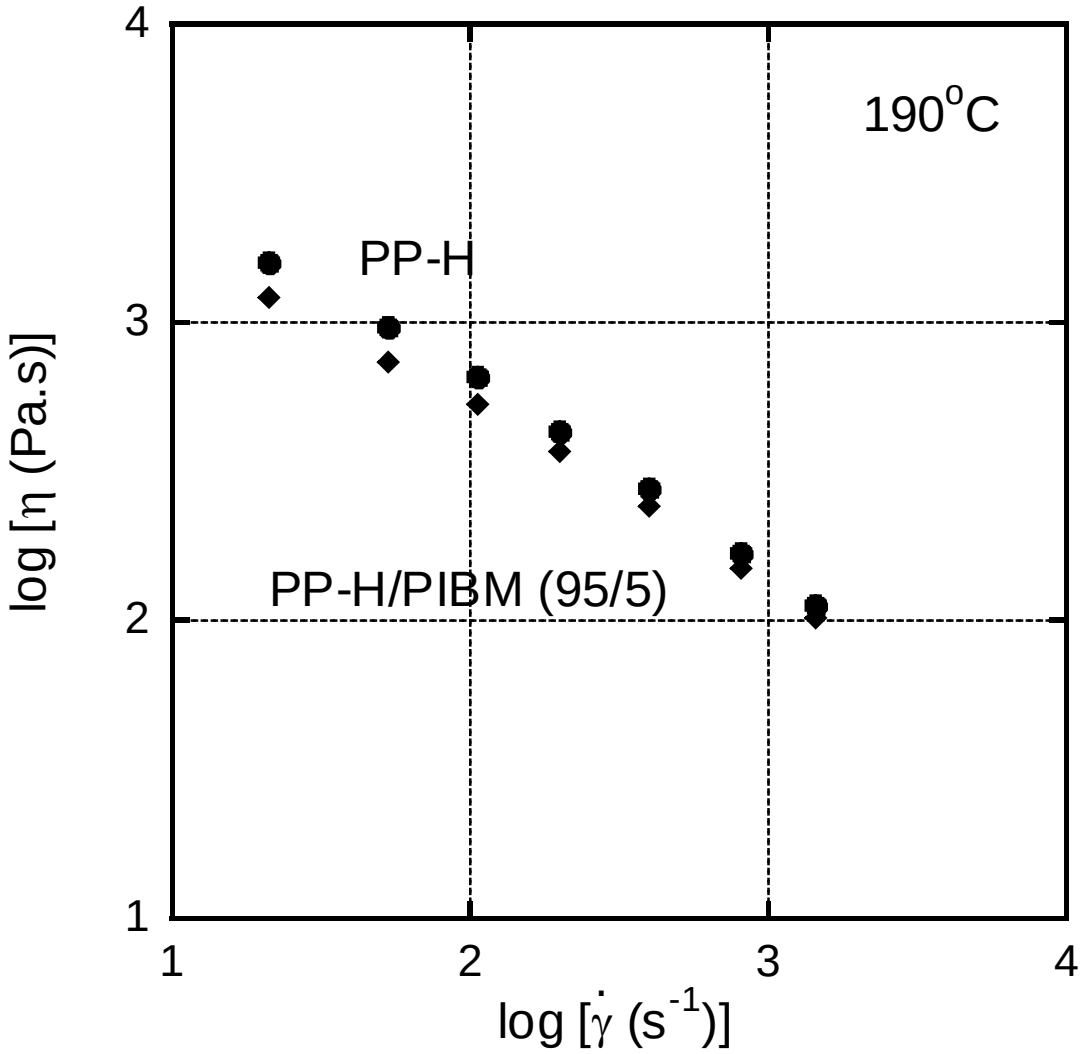

SEEMORK et al., FIG. 4

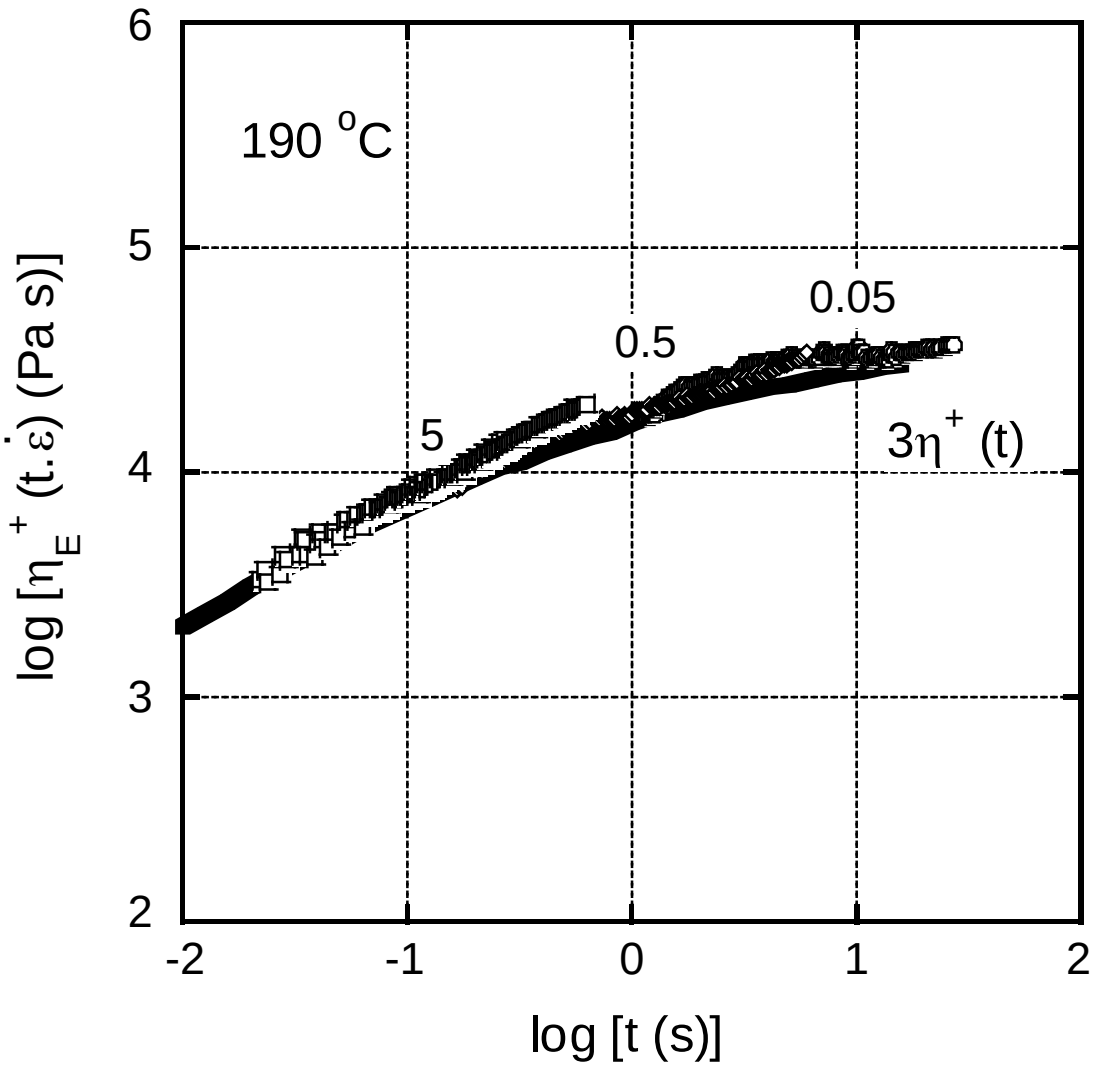

SEEMORK et al., FIG. 5

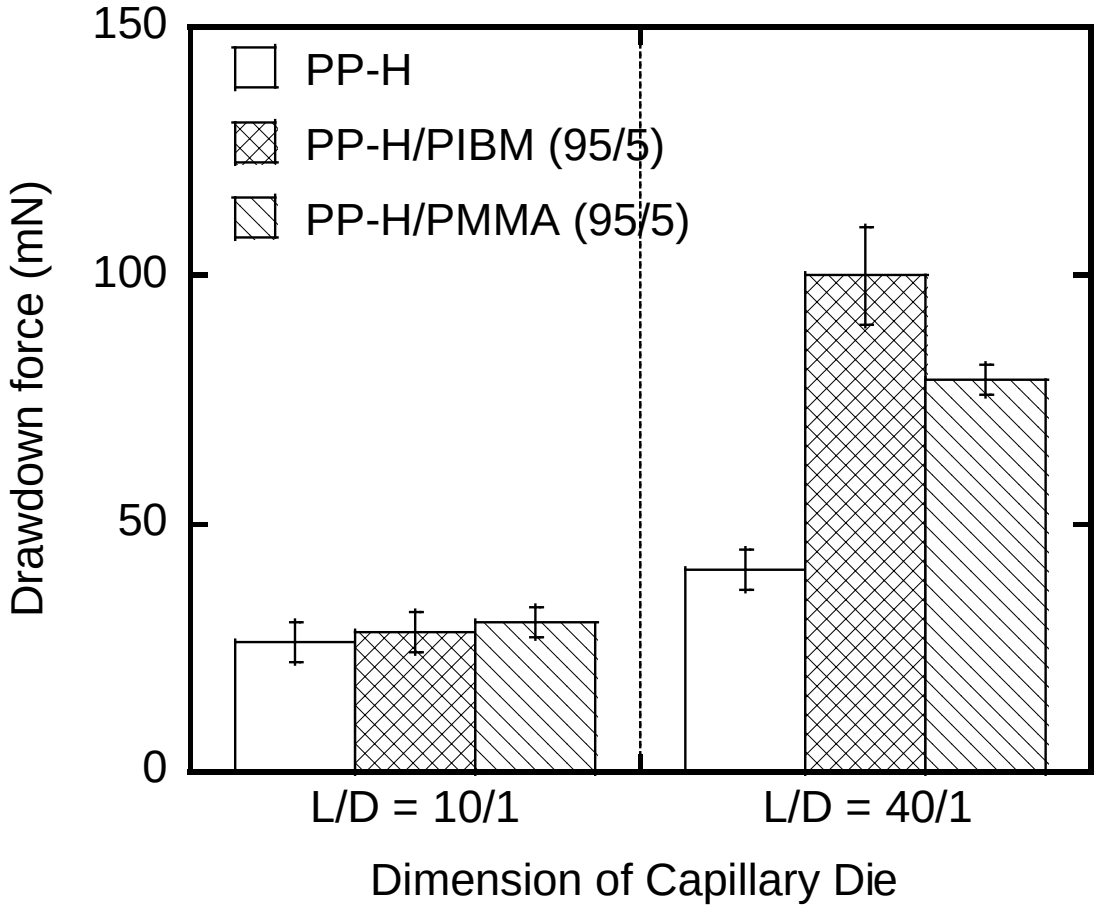

SEEMORK et al., FIG. 6

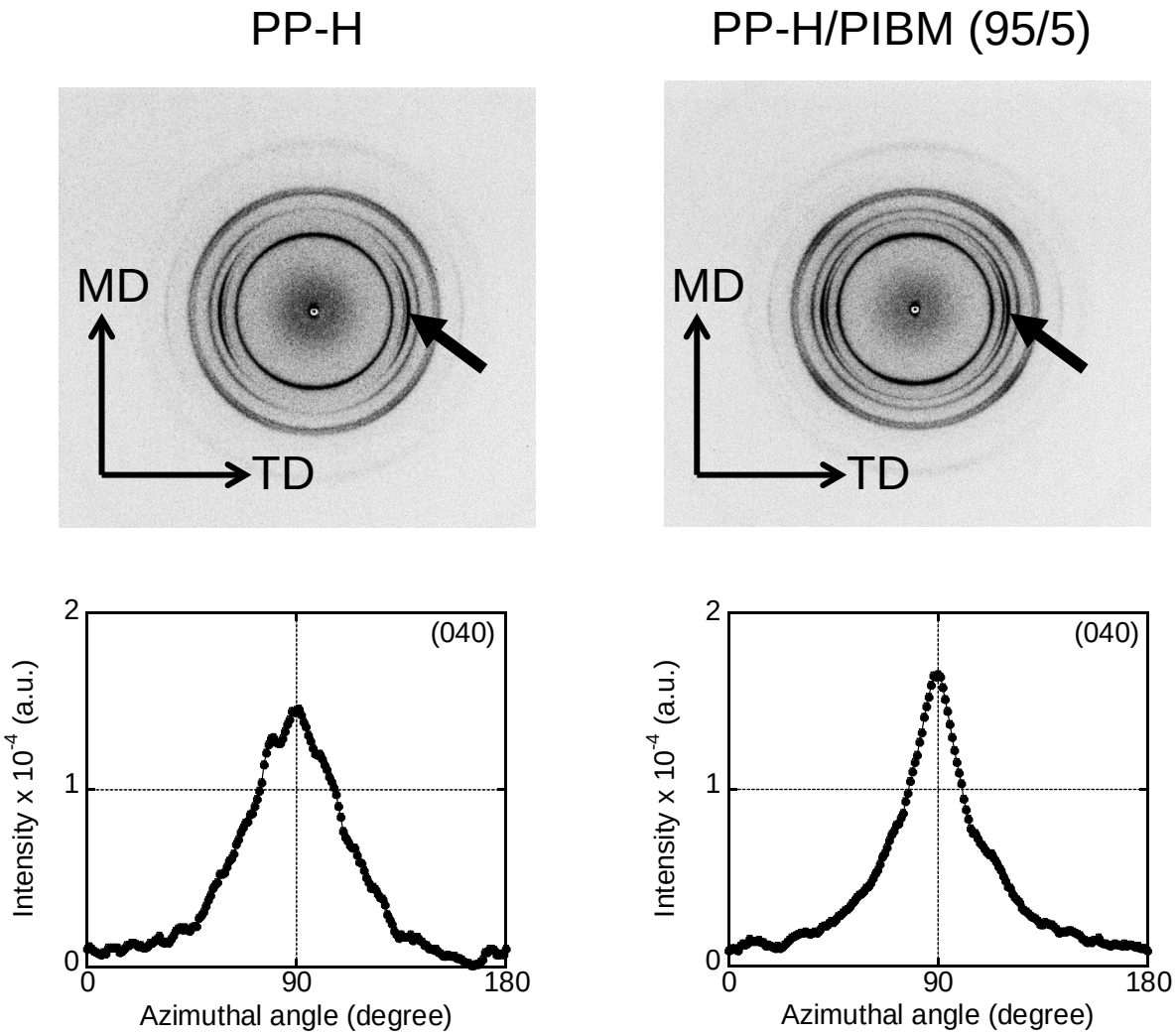

SEEMORK et al., FIG. 7

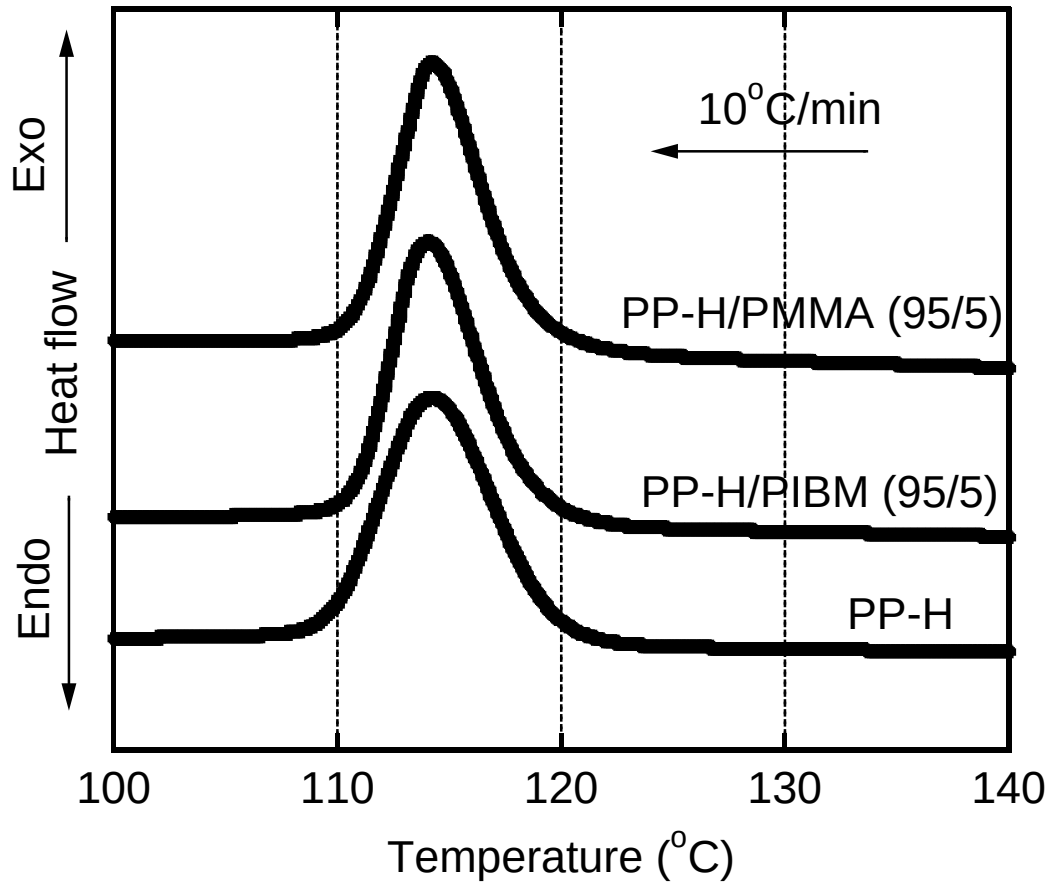

SEEMORK et al., FIG. 8

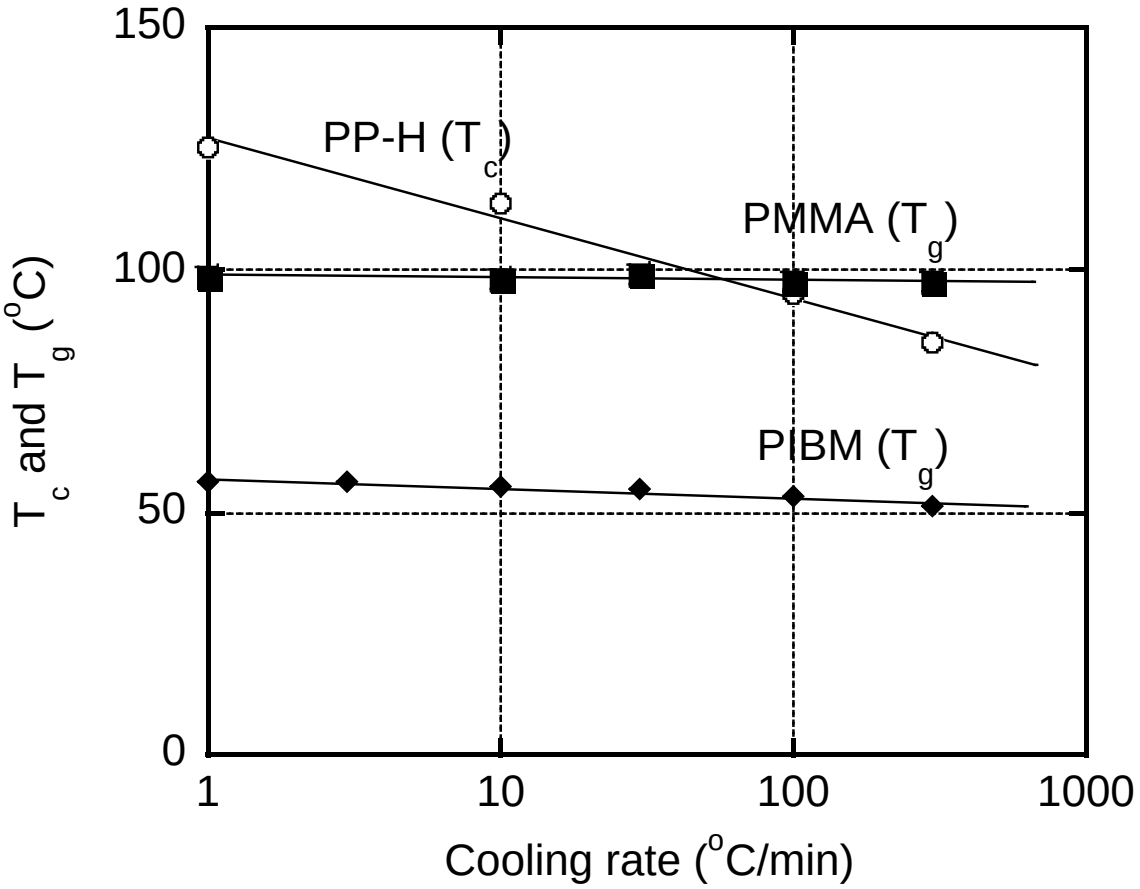

SEEMORK et al., FIG. 9

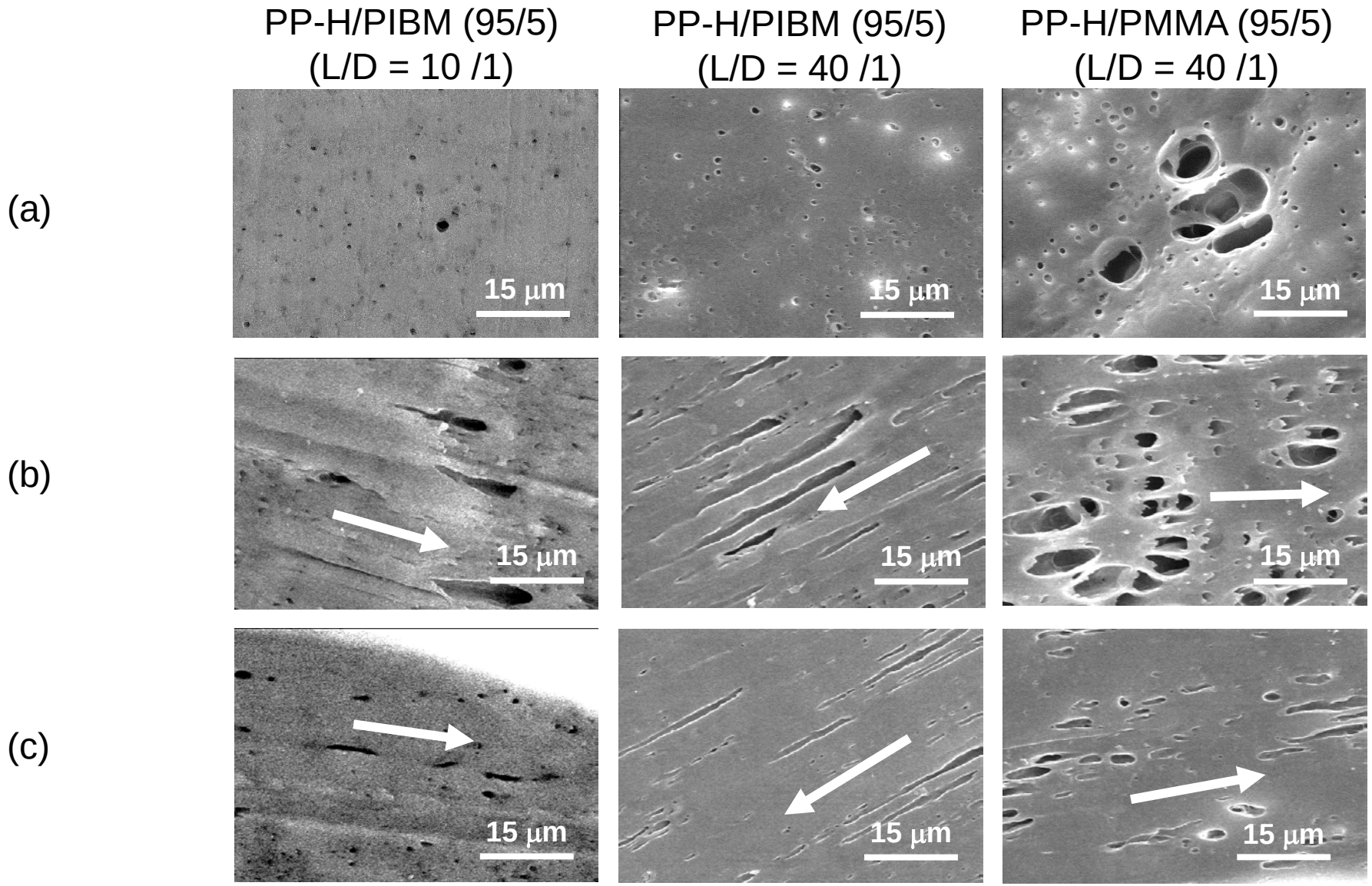

SEEMORK et al., FIG. 10

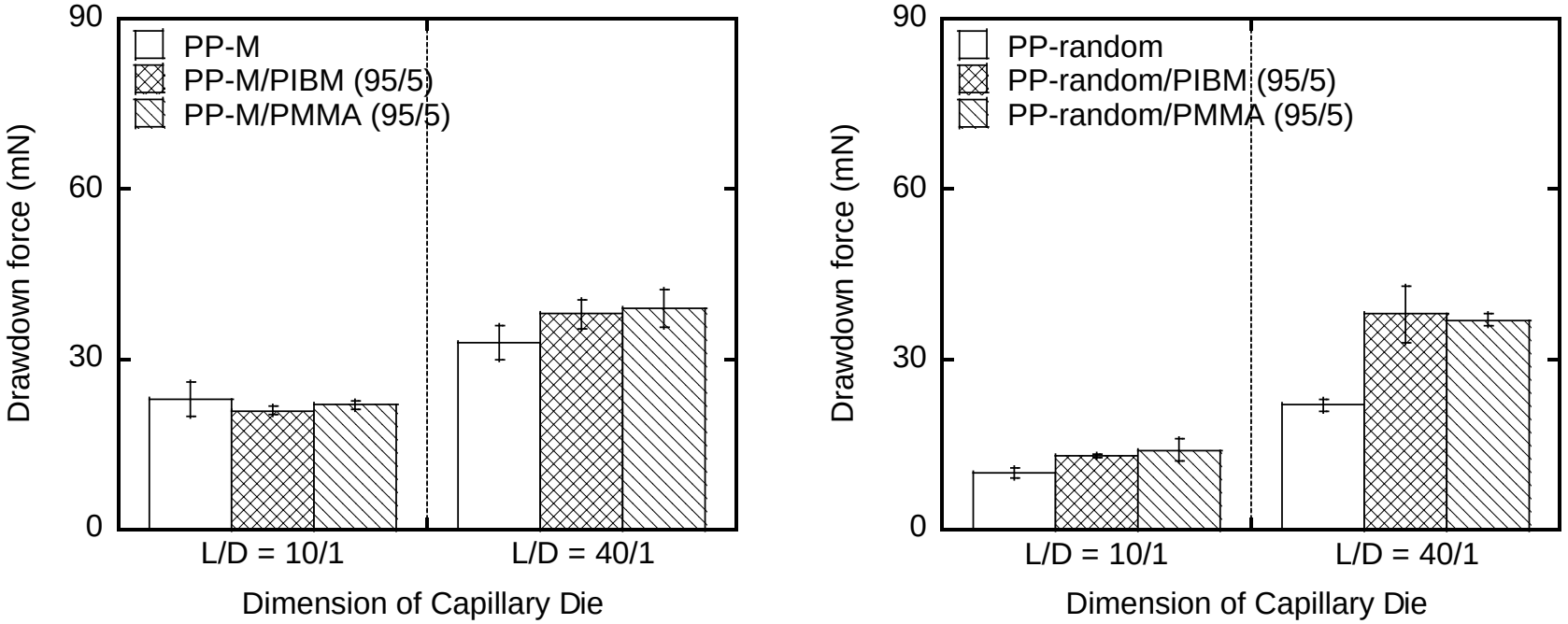

SEEMORK et al., FIG. 11

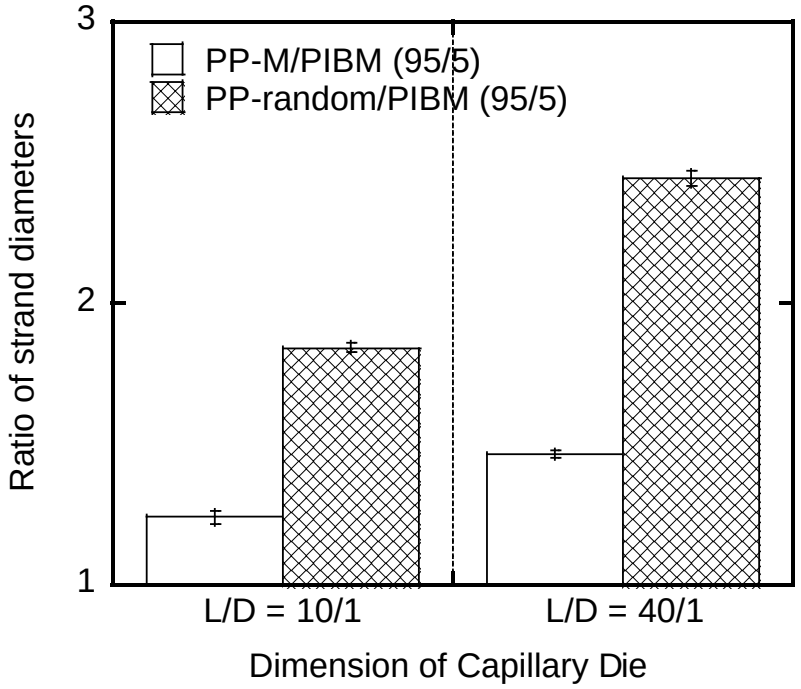

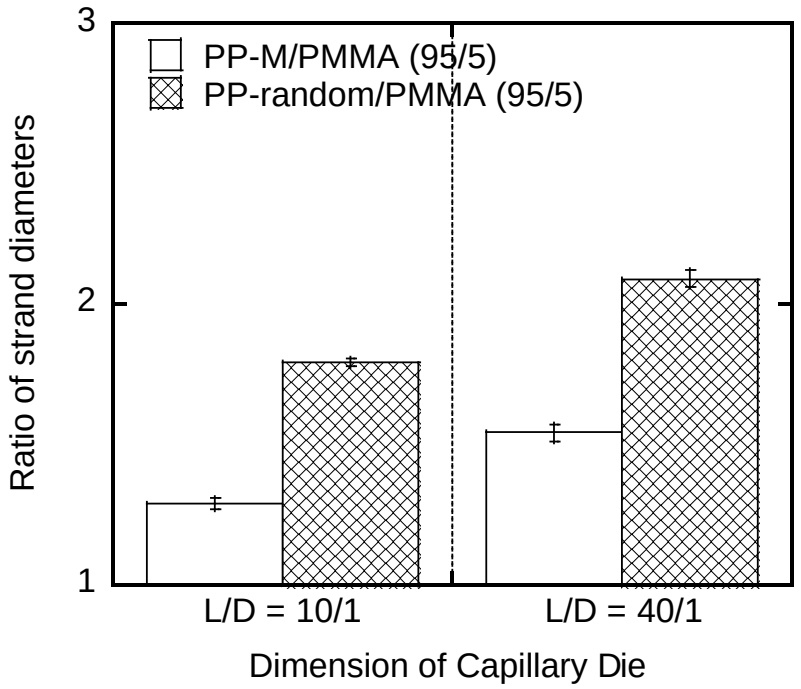

SEEMORK et al., FIG. 12

Table I. Zero-shear viscosity at 190 °C of the materials

Samples	η_0 (Pa s)
PP-H	9,850
PP-M	3,930
PP-random	4,930
PIBM	45
PMMA	280
PP-H/PIBM (95/5)	9,300
PP-H/PMMA (95/5)	9,500

SEEMORK et al., Table I